Pharmaceutical Sciences, 2024, 30(3), 339-354
doi:10.34172/PS.2024.15
https://ps.tbzmed.ac.ir/

Research Article

Lycium barbarum Polysaccharide Attenuates Acute Toxicity Caused by Titanium Dioxide Nanoparticles in Splenic and Pulmonary Tissues

Amal Sewelam[1], Soad L. Kabil[2*], Bashir Jarrar[3], Mohamed Sabry[1], Manal Morsy[1]

[1]*Department of human anatomy and embryology, Faculty of medicine, Zagazig University, Egypt.*
[2]*Department of Clinical Pharmacology, Faculty of Medicine, Zagazig University, Egypt.*
[3]*Nanobiology Unit, College of Science, Jerash University, Jordan.*

Article Info

Article History:
Received: 23 Jan 2024
Accepted: 30 Apr 2024
ePublished: 22 Jun 2024

Keywords:
-Lung
-*Lycium barbarum*
-Oxidative stress
-Spleen
-TiO_2 NPs

Abstract

Background: Titanium dioxide nanoparticles (TiO_2NPs) are widely used in various commercial and industrial applications, posing potential risks to human body. *Lycium barbarum* polysaccharide *(*LBP*)* is renowned for its antioxidant and anti-inflammatory properties. This study aims to investigate the protective potential of LBP against TiO_2 NPs-induced acute toxicity in splenic and pulmonary tissues.

Methods: Forty rats were grouped as follows: Group I, the normal control, received daily 0.1% DMSO intraperitoneally (ip) and 0.5 mL PBS orally. Group II received LBP (100 mg/kg/day) by gavage for 14 days. Group III received a single ip injection of TiO_2 NPs (972 mg/kg) on the 8th day. Group IV obtained both LBP and TiO_2 NPs. Group V was treated with LBP, TiO_2 NPs and Zinc protoporphyrin IX (ZnPPIX), the later was injected ip in a dose of 10 mg/kg/day one hour before LBP. Biochemical, histopathological, and immunohistochemical analysis were conducted on splenic and pulmonary tissues of all rats.

Results: TiO_2 NPs induced congestion, inflammation, macrophage proliferation, pyknosis and significantly increased caspase-3, CD68, NF-κB, TLR4 immunoexpression with upregulation of markers of oxidative stress, inflammation, apoptosis and fibrosis. Pretreatment with LBP mitigated TiO_2 NPs-induced tissue damage but enhanced heme oxygenase-1 (HO-1) mRNA expression. Co-administration of ZnPPIX reversed LBP protective impact.

Conclusion: LBP demonstrated the ability to alleviate splenic and pulmonary injuries caused by the acute TiO_2 NPs toxicity. LBP prevents TLR4/NF-κB mediated injury triggered by TiO_2 NPs through HO-1 upregulation. Further research is required to explore the preventative role of LBP against both acute and chronic toxicity brought by nanomaterials in general and TiO_2 NPs in particular.

Introduction

Titanium dioxide nanoparticles (TiO_2 NPs) have been extensively used in a diversity of consumer products and research applications. They gained great interest based on their unique thermal, optical, electrical, mechanical, and magnetic properties.[1] Therefore, TiO_2 NPs have opened up opportunities in numerous biological, cosmeceutical, pharmaceutical, optical, and commercial fields. They are used in medical devices, drug delivery, disease diagnosis, nanotherapeutics, photocatalysis, food processing and packaging.[2,3] Ingestion and inhalation are considered the most prevalent routes of TiO_2 NPs exposure in humans, in addition to injection and transdermal penetration.[4]

The extensive production, broad application, growing consumption, and uncontrolled disposal of TiO_2 NPs raise questions about whether the risks outweigh advantages.[5] Some in vivo experimental studies established that, TiO_2 NPs can reach, rapidly distribute and accumulate in vital organs triggering oxidative stress as well as tissue and cell damage.[6] Additionally, the injected TiO_2 NPs can rapidly disperse in various tissues and cells, inducing inflammation, cytotoxicity, genotoxicity, and immunotoxicity that might be influenced by NPs size. The smaller the size, the greater the inflammatory response.[7] Further, a dose-response study of acute TiO_2 NPs toxicity verified marked histological insults in various body organs including spleen, lung, kidney, and liver. The spleen has obtained the largest amount of TiO_2 NPs with evident splenic injury.[8] Moreover, severe pulmonary and extrapulmonary inflammation strongly associated with oxidant /antioxidant imbalance was declared.[9] According to reports, the spleen may not only assist in NP clearance but also becomes a key target organ for their pharmacological impact.[10] Oxidative stress elicited by reactive oxygen species (ROS) formed on the

*Corresponding Author: Soad L. Kabil, E-mail: soadkabil2004@gmail.com

surface of TiO_2 NPs makes their extensive use a reasonable cause for worry.[11]

Heme oxygenase-1 (HO-1) exerts a masterful role in oxidative stress fighting and maintenance of cellular homeostasis.[12] Heme degradation is catalyzed via HO-1 into biliverdin, carbon monoxide (CO) and free iron. All HO-1 products mediate cytoprotection as they scavenge ROS.[13] Significant anti-apoptotic and anti-inflammatory impacts are enhanced by CO. Furthermore, CO suppresses the manufacture of pro-inflammatory cytokines.[14]

Toll like receptor (TLR)-4 is a master pathway involved in induction of the innate immune response and cellular inflammation.[15] Also, TLR4 can induce host inflammatory responses mediated via macrophages, neutrophils, and complement. Further, TLR4 stimulation triggers the activation of many pro-inflammatory cytokines and chemokines.[16] Nuclear Factor Kappa B (NF-κB) is a downstream target mediated by TLR4.[17] Myeloid differentiation 88 (MyD88) is a widely expressed cytoplasmic inflammatory adaptor protein. It is one of the essential downstream proteins of TLR4.[18] Earlier studies documented the relationship between HO-1 and TLR4-mediated signaling. Overexpression of HO-1 downregulates TLR4 expression and thus alleviates liver damage in cases of hepatic ischemia reperfusion injury.[19]

Lycium barbarum polysaccharide *(*LBP*)* is a well-known traditional Chinese medicinal derived from the wolfberry fruits. The anti-inflammatory, immunomodulatory, antioxidant, anti-aging, anticancer, and neuroprotective properties are essential characteristics of LBP.[20] Previous investigations revealed LBP- protective impact against lung injury based on its ability to suppress inflammation, ROS generation, as well as its role in enhancing antioxidant status.[21] Additionally, LBP can promote the immune organs with subsequent enrichment of the host immunity.[22] Furthermore, LBP influences the activity of B-lymphocytes, T-lymphocytes, and macrophages, as well as its capability to attenuate the inflammatory immune response and pro-inflammatory cytokine release.[23] Previous studies reported a positive regulatory role of LBP on nuclear factor erythroid 2–related factor 2 (Nrf2) / HO-1 signaling.[24] Additionally, LBP inhibited TLR4, MyD88, and NF-κB expressions in aged mice exposed to ovariectomy-mediated cognition distraction.[25] Moreover, LBP enhanced the immunomodulatory impact against hepatic fibrosis and downregulated fibrosis gene expression.[26]

The current study aimed to elucidate the potential protective role of LBP against TiO_2 NPs-mediated biochemical, histological, and immunohistochemical derangements of the spleen and lung. Also, to explore the incorporation of HO-1 signaling and TLR4 / NF-κB pathway in such protection.

Methods

Chemicals

Titanum dioxide nanoparticles (TiO_2NPs) composed of titanium (IV) dioxide NPs, anatase which was purchased from Sigma-Aldrich, Egypt. It has a purity of 99.7%; an average particle size of 25-nm and a surface area of 45–55 m^2 /gm. The Nano-powder was dispersed in normal saline (NaCl, 0.9%) for 20 min at room temperature just before injection.[27] LBP was purchased from (Xi'an Natural Field Bio-Technique Company, Ltd., Shanxi, China) with a purity of 51.87%. Zinc protoporphyrin IX (ZnPPIX) is HO-1 inhibitor which provised from Wako Pure Chemical Industries, Osaka, Japan.

Experimental animals

Forty healthy adult male Wister albino rats aged 9-10 weeks, with a weight of 220±20 g, were bought from Zagazig Scientific Medical and Research Center's animal facility. The animals were caged (n= 4 /cage) within a well-ventilated room under controlled conditions (12h: 12h light/dark cycle, 23± 2°C). The typical laboratory rodent chow pellets and clean water were readily available.

Experimental design

Following a period of 7 days acclimation, all rats under study were randomly allocated into 5 groups (8 rats each) as follow: Group I: served as normal control (NC) group. Each member daily received 0.5 mL phosphate buffered saline (PBS) (vehicle for LBP) via gavage and 0.5 mL of 0.1% dimethyl sulfoxide solution (DMSO) in normal saline (vehicle for ZnPPIX) by ip injection. Additionally, on the 8th day of the study, a single dose of 0.5 mL normal saline was injected ip (vehicle for TiO_2 NPs). Group II (LBP group): each rat received LBP at a dose of 100 mg/kg once/day via gavage for 14 days.[24] Group III (Ti group): each member had a single ip injection of TiO_2 NPs (972 mg/kg) on the 8th day of the study.[8] Group IV (LBP + Ti group): each rat received both LBP and TiO_2 NPs as previous. Group V (LBP+ Ti+ ZnPPIX group): each member obtained both LBP and TiO_2 NPs as previous with the addition of ZnPPIX (10 mg/kg) injected ip once per day, 1h before LBP treatment for 14 days.[28]

Specimens' collection

Rats were anesthetized at the end of the experiment, 24 hours after the last experimental dose, using thiopental ip (50 mg/kg) in compliance with IACUC protocol. For each rat in every group, the spleen as well as both lungs were dissected, extracted, and rinsed with ice-cold saline. Specimens gathered from 4 rats / group were processed for routine histopathological analysis. However, spleen slices as well as left lung samples from the other 4 rats / group were homogenized and processed for biochemical analysis, while 4 right lung samples and 4 spleen biopsies were utilized for quantitative reverse transcriptase polymerase chain reaction (RT-qPCR) analysis.

To achieve 10% homogenates, the obtained tissue specimens were washed with cold PBS (0.01M, Ph 7.4). Homogenization was performed in 180 µL PBS at 4°C. The resultant homogenates were washed with potassium chloride (1.15%) and cold saline 0.9 %. Centrifugation at

10000 xg for 10 min at 4°C was done to remove debris. The supernatants were cooled in an ice bath for 12 min then subdivided to be ready for biochemical assessments.

Malondialdehyde (MDA) assay

MDA level, the lipid peroxidation end product, was measured in the supernatant by using Bio-diagnostic colorimetric assay kit (catalog #: E-BC-K025). MDA react with thiobarbituric acid generating a red colored product with absorbance at 532 nm then compared with the standard curve of MDA tissue concentrations.

Activity of superoxide dismutase (SOD)

SOD tissue activity of the supernatant was assayed based on WST-1 method (catalog #: E-BC-K020, Elabscience Biotechnology Inc.) as follow: xanthine oxidase catalyses WST-1 interact with O_2- generating a hydrophilic formazan dye. SOD catalyzes superoxide anions disproportionation thus inhibiting the reaction. There is a negative correlation between SOD activity and formazan dye amount. SOD activity could be identified through colorimetric analysis of WST-1 products. A change in absorbance at 450 nm was identified.

Reduced glutathione (GSH) assay

Levels of GSH were measured in the obtained supernatant using colorimetric assay kit (catalog #: E-BC-K096, Elabscience Biotechnology Inc). GSH reacts with dithionitrobenzoic acid producing thionitrobenzoic acid and glutathione disulfide. Nitromercaptobenzoic acid has a yellow color with highest absorbance at 420 nm. GSH level could be determined by obtaining the optical density value at 420 nm.

Catalase (CAT) activity

Activity of CAT was determined in the supernatant by the use of colorimetric assay method (catalog #: E-BC-K031, Elabscience Biotechnology Inc). Decomposition of H_2O_2 by CAT can be inhibited by ammonium molybdate. The remained H_2O_2 react with ammonium molybdate giving a yellow colored complex. The activity of CAT was determined by generation of the previously mentioned complex at 405 nm.

Assay of transforming growth factor β1 (TGF-β1)

In order to estimate tissue protein levels of the fibrosis marker TGF-β1, ELISA kit (catalog #: MBS702305 MyBioSource) was utilized. The microtiter plate was pre-coated with TGF-β1 specific antibody. Samples and standards were added to the specific microtiter plate wells together with a biotin conjugated antibody sensitive to TGF-β1. Additionally, Avidin with Horseradish peroxidase was inoculated with the wells. After that, tetramethyl-benzidine was added. Biotin inoculated antibody reacts with avidin enzyme complex produce a change in color only in the presence of TGF-β1. Sulphoric acid solution was used to stop the reaction. The color alteration was identified spectrophotometrically at 450 ± 2 nm. TGF-β1 concentration was determined by comparing the optical density of the samples with the regular curves.

Assay of anti-apoptotic marker B-cell lymphoma 2 (Bcl-2)

Bcl2 tissue levels were estimated by using the sandwich ELISA technique based on an ELISA kits purchased from MyBioSource.com (catalog #: MBS2515143). The plates were inoculated with antibody relevant to rat Bcl2. The supernatant samples and standards were added to the plates. Biotinylated antibody against Bcl2 with Avidin Horseradish peroxidase conjugate was incubated with the wells. After washing, the test samples were added to every well. A blue color appeared only in wells containing Bcl2. To terminate the reaction of enzyme and the substrate, add stop solution and the color back to yellow. Bcl2 concentration is assayed spectrophotometrically at wavelength 450 ± 2 nm by detection of the optical density and comparing it to the standard values.

Assay of pro-apoptotic marker BCL2 associated X (Bax)

This assay was performed by use of sandwich ELISA principle (catalog #: E4513, BioVision-Abcam). The microtiter plates were pre-coated with the specific antibody targeting Bax. Both standards and test samples were added to the plates. The antigen bound with its target antibody. Wasting was done to remove the unbound standard or test samples. Detection biotin antibody was added to bind the antigen. Avidin horseradish peroxidase (HRP) conjugate was added to catch biotin. TMB solution was added with subsequent reaction with HRP enzyme leading to a color change. Stop solution was added to terminate the reaction. The optical density (OD) of the wells was measured at 450± 2 nm and OD of Bax in samples was determined in respect to OD standard curve.

Myeloid differentiation 88 (MyD88) assay

Sandwich enzyme immunoassay ELISA kit (catalog #: MBS2703631, MyBioSource.com) was used to estimate the inflammation marker, MyD88. An antibody specific for MyD88 was incubated with standards and samples in microplates. Biotin inoculated antibody targeting MyD88 was added. Incubation with Avidin- Horseradish peroxidase was made. Then, TMB substrate was added to the wells and a change in color took place in wells containing MyD88 only. Sulphoric acid terminated the reaction. MyD88 concentration was determined spectrophotomerically at 450 ±10 nm wavelength referred to OD of the samples of standard curve.

RT-qPCR

Total RNA was extracted from four right lung samples and spleen biopsies using Trizol (Invitrogen; Thermo Fisher Scientific, Inc.). For RNA isolation and complementary DNA (cDNA) synthesis, the RNeasy Mini kit, including DNase I treatment, were applied following the manufacturer's protocols (QIAGEN, #74104).RNA was then reversed

transcribed using Quant Script reverse transcriptase (QuantiTect Reverse Transcription Kit, QIAGEN). RT-qPCR was performed using specific primers for rat HO-1, and Glyceraldehyde 3-phosphate dehydrogenase (GAPDH) that was utilized as a reference gene to estimate fold change in target gene (HO-1) expression. For both spleen and lung, the specific primer sequence was the same as follow: HO-1 (F: 5'AAGAGGCTAAGACCGCCTTC-3', R: 5'GCATAAATTCCCACTGCCAC-3'; GAPDH (F: 5'ACGGCAAGTTCAACGCACAG-3', R: 5' GAAGACGCCAGTAACTCCAGAC-3'). The RT product was amplified in a volume of 10 µL containing 2 µL cDNA, 2 µL RNAse-free water, 5 µL SYBR Green master mix (Roche Diagnostics) and 0.5 µL of each primer (10 pmol / µL). After an initial 20 seconds at 95°C, 40 cycles of 3 seconds at 95°C and 30 seconds at 60°C were performed. The expression level of HO-1 mRNA in both spleen and lung was normalized to GAPDH.

Histological processing

For routine handling and processing of paraffin blocks for histological and immunohistochemical analysis by light microscope, the selected spleen and lung specimens were immersed and fixed using 10 % neutral buffered formalin for a period of 24-72 hours. Instillation of fixative through syringes inserted into the airways of the lung was performed. After that, dehydration in ascending grades of ethanol, clearance, paraffin impregnation and blocking were achieved. Lastly, serial Paraffin sections (4 µm thick) were processed and subjected to staining. Dewaxing, rehydration, mounting on slides and dying with Hematoxylin and eosin (H&E) stains were applied to demonstrate the routine histological construction of the spleen and lung. Also, Masson's Trichrome (MT) stain was applied to demonstrate the collagen fiber content to evaluate fibrosis.[29]

Immunohistochemical analysis

To determine the transcription of caspase-3, CD68, NF-κB and TLR4 proteins in both spleen and lung paraffin sections, the peroxidase-labeled Streptavidin—Biotin Technique was carried out for immunohistochemical (IHC) staining in accord with procedures described by Torlakovic *et al.*[30] Briefly, 4µm spleen and lung paraffin slices were mounted on positive charged slides, dewaxed, rehydrated and finally subjected to endogenous peroxidase activity blocking (using 3% H_2O_2 in PBS for 30 min). Then immersion in antigen retrieval solution and then incubation in 10% normal goat serum in BPS for nonspecific antigen blocking were accomplished. Afterward, in a humid chamber at 4°C, the slides were incubated separately overnight with solutions of different primary antibodies. Apoptosis marker (Caspase-3): rabbit polyclonal antibody (PA1-26426, Fisher scientific, Lab Vision Corporation Laboratories). Macrophage marker (CD68): rabbit Polyclonal antibody (Cat. No.: E-AB-64533, Elabscience, Lab Vision Corporation, Neomarkers Laboratories, Westinghouse, Thurmont, California, USA). Inflammation marker (NF-kβ, Nuclear Factor kappa light chain enhancer of activated β cells): a rabbit polyclonal antibody (ab86299, Abcam, Cambridge, Massachusetts, USA). Toll-like receptor 4 (TLR4): mouse monoclonal antibody (ab22048, Abcam, Inc Cambridge, UK). Next, the slides were washed in PBS, incubated with biotinylated secondary antibody for 2 h at room temperature, and then washed again in PBS. Streptavidin peroxidase supplementation for 10 min, diaminobenzidine (DAB)-hydrogen peroxide application, and finally Mayer's hematoxylin counterstaining were accomplished. To confirm staining validity, negative control slices were prepared in the same steps but with replacement of primary antibody by PBS. Positive reactions were considered in cells that displayed brown precipitate. The immune-stained slices were inspected to capture immunoreactivity using a light microscope (Leica Microsystem, Schweiz, AG, Heerbrugg, CH-9435, Switzerland).

Morphometric measurements

Collagen deposit, caspase 3, NF-κB, and TLR4 positive immune expression area percentages were calculated. CD68 immunopositive macrophages were also counted. The study was performed using FIJI/ Image J® software (1.51 n; National Institute of Health, Bethesda, USA). The analysis was achieved using 3 sections / rat × 400 magnification (4 rats / group) in all study groups. Data were subjected to statistical analysis.[31]

Statistical analysis

First, all datasets were assessed for normality. Subsequently, the quantitative biochemical and histomorphometry data were computerized and statistically evaluated using GraphPad Prism, Version 9.2 (GraphPad Software Inc., San Diego, California, USA). Quantitative data were expressed as mean ± SD. ANOVA was applied to determine any significant differences among mean values of different study groups. In addition, Tukey's multiple comparison test was carried out as a post hoc test of ANOVA.

Results

There were no discernible structural or statistically significant ($p>0.05$) differences between the normal control and LBP-treated groups. So, for comparisons with other study groups, the control group was thus used.

LBP alleviated TiO_2 NPs-induced oxidative stress and fibrosis

As illustrated in Tables 1, 2 TiO_2 NPs exposure significantly ($p<0.05$) increased TGF-β1, MDA while simultaneously decreasing GSH, SOD, CAT activities compared with control group. Conversely, LBP pre-treatment induced a significant ($p<0.05$) decline in TGF-β1, MDA coupled with a notable increase in antioxidants activities when contrasted with Ti group. Notably, ZnPPIX co-administration significantly ($p<0.05$) reversed LBP beneficial effects

Table 1. Effect of LBP and co-administration of ZnPPIX on oxidative stress and fibrosis markers in TiO_2 NPs-induced splenic injury.

Groups (n=8)	NC	LBP	Ti	LBP+ Ti	LBP + Ti + ZnPPIX
MDA (nmol/g tissue)	1.29 ± 0.22	1.16±0.02	3.03 ± 0.20*	1.59 ±0.30#	2.98 ± 0.25$
SOD (U/g tissue)	56.33 ±3.38	51.65±4.26	34.67 ±3.07*	46.00 ±4.05#	39.00 ±3.16$
GSH (µmol/g tissue)	82.39±4.01	78.41±4.35	26.58±3.06*	57.41±5.73#	30.36±4.42$
CAT (U/mg tissue)	10.40 ±0.92	11.3±2.4	5.85 ±0.62*	8.31± 0.76#	6.06± 0.67$
TGF-β1 (pg/mg tissue)	16.83±1.47	17.67±1.21	46.33±4.13*	22.5±2.73#	40.33±3.50$

NC: normal control; LBP: *Lycium barbarum* polysaccharide; Ti: TiO_2 NPs (titanium dioxide nanoparticles); MDA: malondialdehyde; SOD: superoxide dismutase; GSH: glutathione; CAT: catalase; ZnPPIX: zinc protoporphyrin IX; TGF-β1: transforming growth factor- β1. Data represent mean ± SD; *p < 0.05 significant vs.NC; #p < 0.05 significant vs. Ti group; $p< 0.05 significant vs. (LBP+ Ti) group.

Table 2. Effect of LBP and co-administration of ZnPPIX on oxidative stress and fibrosis markers in TiO_2 NPs-exposed pulmonary injury.

Groups (n=8)	NC	LBP	Ti	LBP +Ti	LBP + Ti + ZnPPIX
MDA (nmol /g tissue)	8.25 ± 0.92	8.60±1.21	39.50 ±1.12*	12.50 ±0.86#	24.80 ±1.37$
SOD (U/g tissue)	12.63±0.82	12.61±0.9	4.31 ± 0.80*	10.05 ± 0.84#	7.06 ± 0.72$
GSH (µmol /g tissue)	69.02±5.76	66.73±2.99	24.91±2.85*	58.81±4.47#	31.05±5.69$
CAT (U/mg tissue)	34.15± 1.44	32.38±0.4	11.18 ± 1.03*	25.97 ± 1.80#	17.53 ±1.66$
TGF-β1 (pg /mg tissue)	18.50 ±2.42	18.67 ±3.14	49.67 ±5.78*	21.67± 3.38#	45.00± 4.00$

NC: normal control; LBP: *Lycium barbarum* polysaccharide; Ti: TiO_2 NPs (titanium dioxide nanoparticles); MDA: malondialdehyde; SOD: superoxide dismutase; GSH: glutathione; CAT: catalase; ZnPPIX: zinc protoporphyrin IX; TGF-β1: transforming growth factor- β1. Data represent mean ± SD. *p < 0.05 significant vs. NC group; #p < 0.05 significant vs. Ti group; $p< 0.05 significant vs. LBP+ Ti group

compared to LBP +Ti group. These findings suggested a correlation between HO-1 and anti-antioxidant, anti-fibrotic properties of LBP.

LBP mitigated TiO_2 NPs triggered apoptosis

As depicted in (Figure 1(A)-(F)),TiO_2 NPs triggered apoptosis in both spleen and lung manifested as a considerable reduction in Bcl-2, Bcl-2/Bax ratio, while a simultaneous rise in Bax ($p<0.05$) relative to the control group. Intriguingly, pretreatment with LBP led to a significant upregulation in Bcl-2, Bcl-2/Bax ratio, and a downregulation in Bax relative to Ti group ($p<0.05$). Yet, the aforementioned parameters were significantly ($p<0.05$) reversed following ZnPPIX co-administration. Such findings proposed the involvement of HO-1 in LBP anti-apoptotic influence.

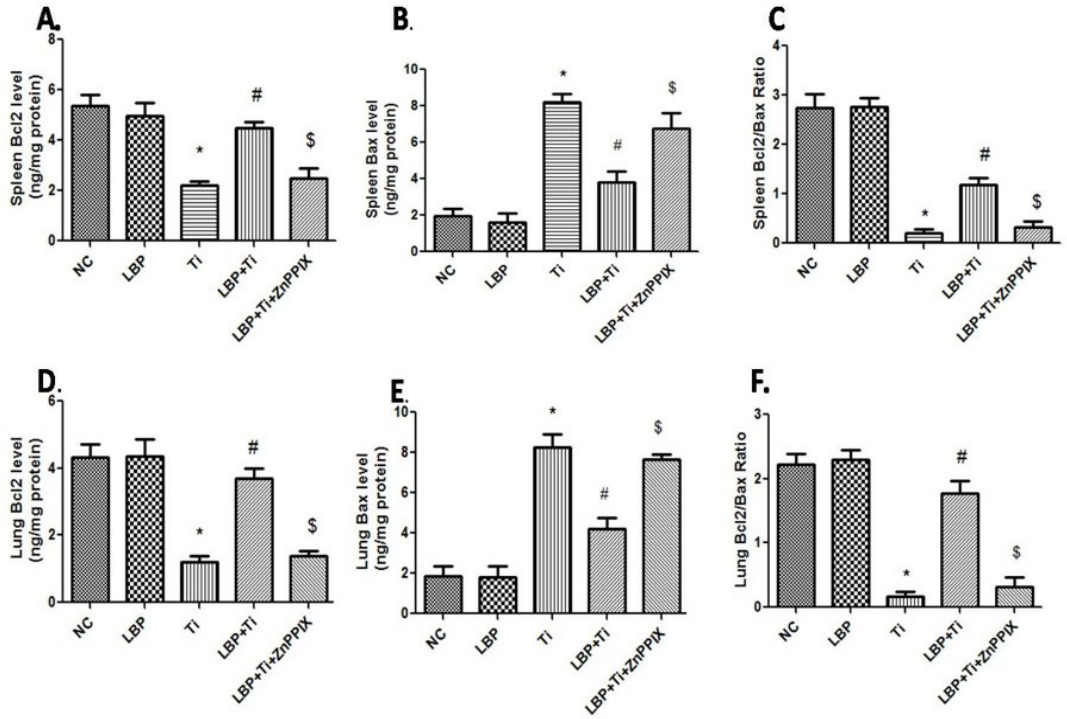

Figure1. Effect of LBP pretreatment and ZnPPIX co-administration on apoptosis markers in rats' spleen (A-C) and lung (D-F) exposed to TiO_2NPs. NC: normal control group; LBP: *Lycium barbarum polysaccharide*; Ti: TiO_2NPs; ZnPPIX: zinc protoporphyrin IX. Data are represented as Mean ± SD, *p < 0.05 significant vs. NC; # p < 0.05 significant vs. Ti group; $p< 0.05 significant vs. LBP +Ti group.

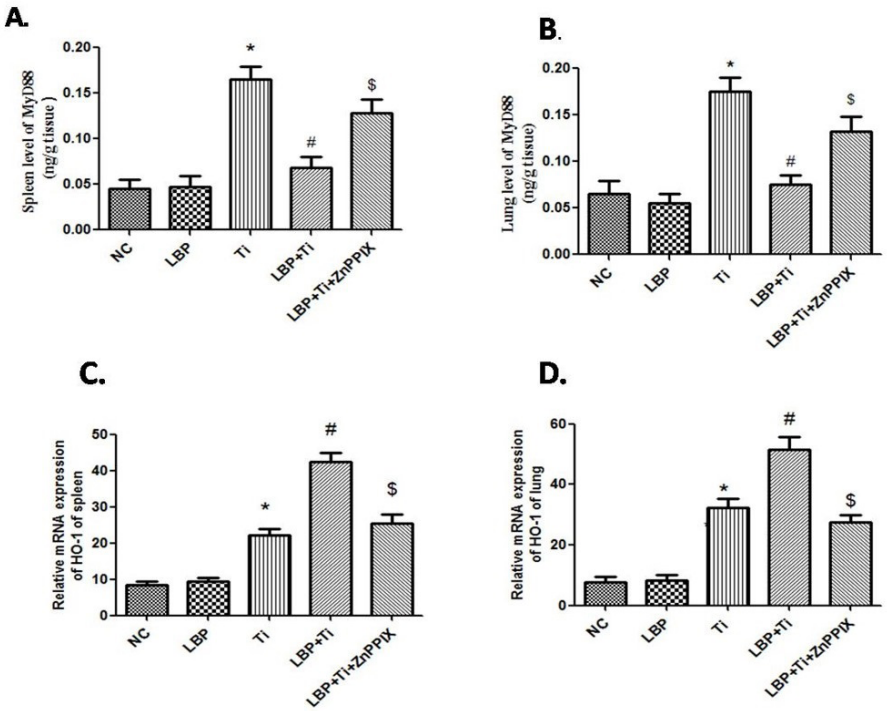

Figure 2. Effect of LBP and ZnPPIX co-administration on MyD88 level and HO-1 mRNA expression in rats' spleen (A)-(C) and lung (B)-(D) exposed to TiO_2 NPs. MyD88: myeloid differentiation primary response 88; HO-1: heme oxygenase -1; NC: normal control group; LBP: *Lycium barbarum polysaccharide*; Ti: TiO_2NPs; ZnPPIX: zinc protoporphyrin IX. Data are represented as Mean ± SD.*p < 0.05 significant vs. NC, #p < 0.05 significant vs. Ti group. $p< 0.05 significant vs. LBP+ Ti group.

LBP alleviated TiO_2 NPs-induced inflammation

As demonstrated in (Figure 2 (A)-(B)), TiO_2 NPs induced inflammation manifested as a substantial ($p<0.05$) rise in MyD88 relative to the control group. Fortunately, LBP pretreatment elicited a substantial ($p<0.05$) MyD88 decline. Co-administration of ZnPPIX considerably ($p<0.05$) raised MyD88 once more. Such findings suggested HO-1 participation in LBP anti-inflammatory impact.

LBP upregulated relative HO-1-mRNA expression

As illustrated in (Figure 2 (C)-(D)), TiO_2 NPs persuaded a significant ($p<0.05$) upregulation of HO-1 mRNA expression relative to the control group with further increase following LBP pretreatment. Nevertheless, ZnPPIX co-administration led to a significant ($p<0.05$) downregulation relative to LBP+ Ti group.

LBP improved TiO_2 NPs induced splenic histological alterations

Hematoxylin and eosin-stained spleen sections retrieved from control (Figure 3 (A-C)) and LBP-treated (Figure 3(D-F)) groups demonstrated normal structure. Alternatively, Ti group (Figure 3 (G-I)) displayed significant splenic damage, shown as white pulp shrinkage, ill-defined marginal zones, deformed central arterioles, splenocytes' nuclear pyknosis, sinus congestion and dilatation, diffuse lymphocytic infiltration, numerous megakaryocytes, and abundant hemosiderin-laden macrophages. LBP pretreatment resulted in a significant improvement. The white pulps restored average size. Also, white, red pulp boundary was obvious. Further, sinuses were less congested, lymphocytic infiltration was diminished, and megakaryocytes were reduced (Figure 3(J-L)). However, some tingible body macrophages (TBMs) were noticed in the white pulps. Conversely, as shown in (Figure 3 (M-O)), ZnPPIX addition reversed LBP elicited histological improvement, with histological findings more or less similar to that in the Ti group.

LBP improved TiO_2 NPs induced pulmonary histological alterations

Lung H&E-stained sections retrieved from both the control (Figure 4 (A-B)) and LBP-treated (Figure 4 (C-D)) groups revealed normal construction. In contrast, TiO_2 NPs exhibited significant degenerative changes such as numerous collapsed alveoli, diffuse interstitial inflammatory cell infiltration, congested pulmonary vessels (Figure 4E); disfigured bronchioles (Figure 4F); extensive intra-alveolar inflammatory cell infiltrate (Figure 4G); numerous intra-alveolar foamy macrophages (Figure 4H). Luckily, LBP-pretreated lung sections displayed marked improvement, as depicted in (Figure 4 (I-J)). Yet, ZnPPIX co-administration reversed LPB elicited improvement and presented massive destructive changes once again (Figure 4 (K-N)).

LBP mitigated TiO_2 NPs induced excess collagen deposition

Sections stained with MT exhibited green colored collagen deposited around splenic vessels (Figure 5 (A-E)),

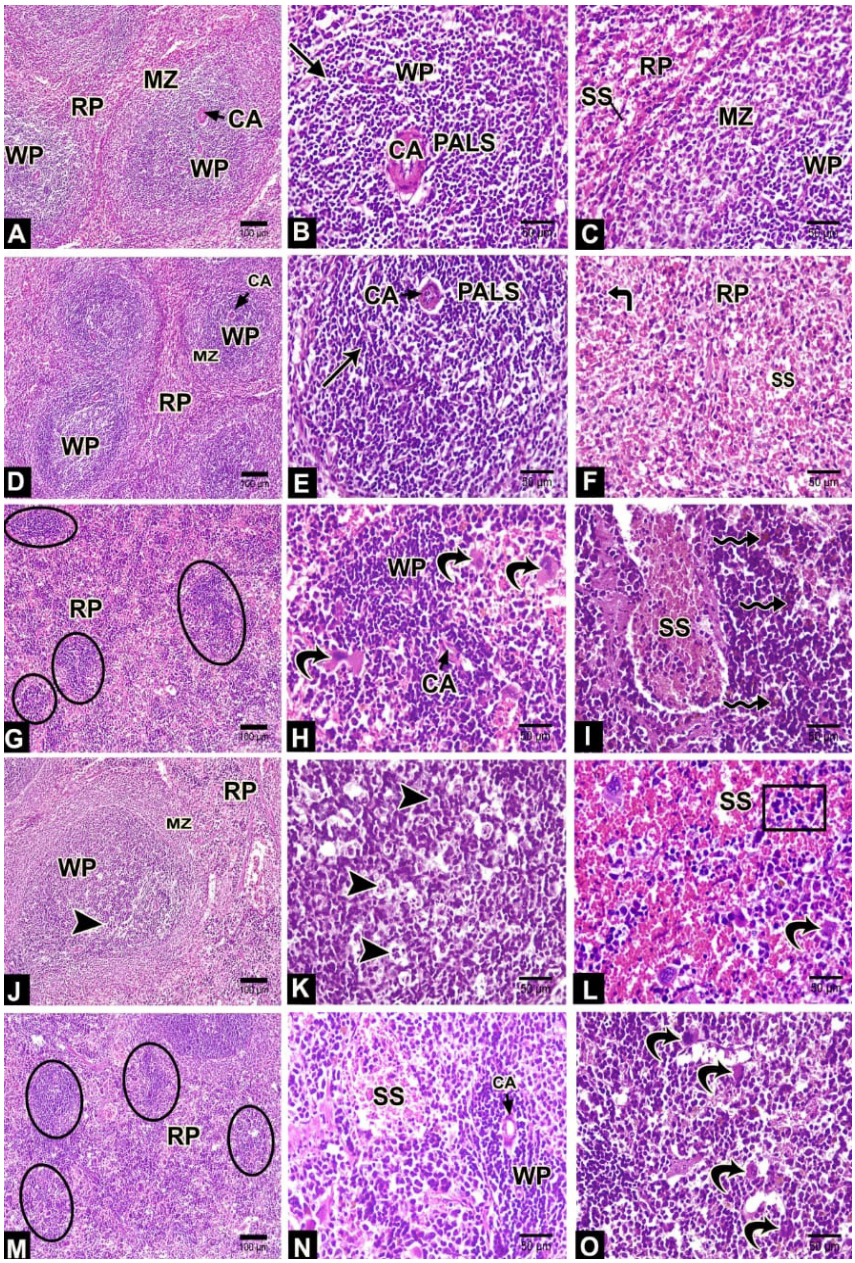

Figure 3. Photomicrographs of H&E stained spleen sections. (A-C) Normal control group. (D-F) LBP group, both display normal white pulp (WP), red pulp (RP), clear marginal zone (MZ), condensed lymphocytes (arrow), central arteriole (CA), periarteriolar lymphatic sheath (PALS), splenic sinuses (SS) and cords (angled arrow). (G-I) Ti group with shrunken white pulps (circle), splenocytes pyknosis, deformed central arterioles (CA), numerous megakaryocytes (curved arrow), sinus congestion and dilatation (SS), diffuse lymphocytic infiltration, abundant hemosiderin laden macrophages (zigzag arrow). (J-L) LBP + Ti NPs group shows average sized white pulps, obvious marginal zones (MZ), less congested sinuses (SS), less lymphocyte infiltration (rectangle), reduced megakaryocytes (curved arrow). However, some tingible body macrophages (TBMs) (arrowhead) are noticed in white pulps. (M-O) LBP + Ti + ZnPPIX group shows deformed shrunken white pulps (circle),tinny central arteriole (CA), dilated congested sinuses (SS), excess lymphocytic infiltration, multiple megakaryocytes (curved arrow). H&E ×100 (A, D, G, J, M); × 400 (B, C, E, F, H, I, K, L, N, O). NC: normal control group; LBP: *Lycium barbarum polysaccharide*; Ti: TiO_2NPs; ZnPPIX: Zinc protoporphyrin IX.

bronchioles and pulmonary vessels (Figure 5 (G-K)). The collagen was relatively little in amount in both control and LBP groups, significantly increased and widely distributed in Ti group. LBP pretreatment induced an obvious reduction in collagen amount. Conversely, ZnPPIX co-administration significantly reversed LBP amelioration with excess collagen deposits again. These findings were further substantiated by estimating the collagen area % as shown in (Figure 5 (F-L)).

LBP decreased protein transcription of caspase-3, CD68, NF-κB and TLR4

In the different study groups, Caspase-3 immunostained spleen and lung sections shown in (Figure 6 (A-E); Figure 6 (G-K)); CD68 immunostained spleen and lung sections shown in (Figure 7 (A-E); Figure 7 (G-K)); NF-κB immunostained spleen and lung sections depicted in (Figure 8 (A-E); Figure 8 (G-K)); TLR-4 immunostained spleen and lung sections depicted in (Figure 9 (A-E);

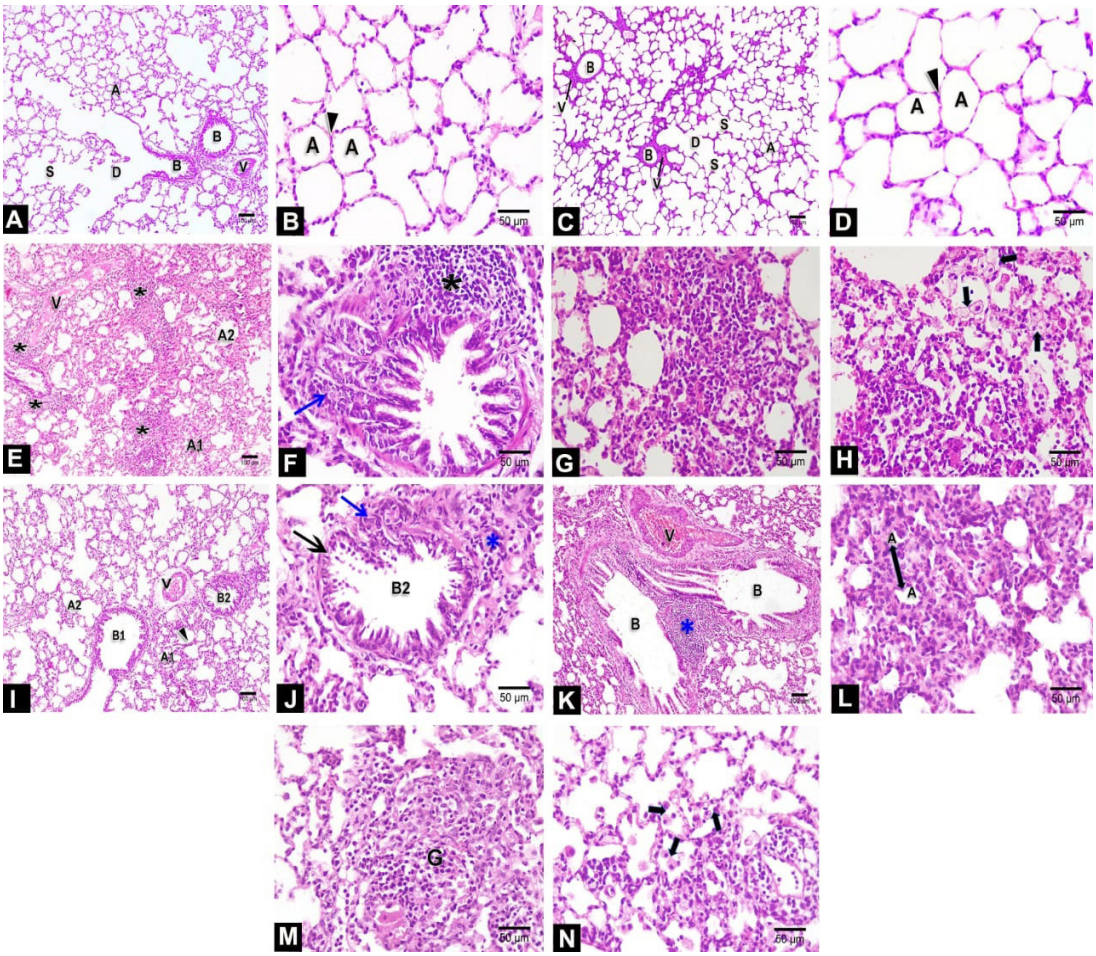

Figure 4. Photomicrographs of H&E stained lung sections.(A-B) NC group. (C-D) LBP group, both show normal bronchioles (B), pulmonary vessels (V), alveolar ducts (D) alveolar sacs (S), alveoli (A) and thin interalveolar septa (arrowhead). (E-H) Ti group. (E) Shows excess collapsed alveoli (A1), few dilated ones (A2), interstitial inflammatory cell infiltrate (*), congestion (V). (F) Shows disfigured bronchiole with epithelial hyperplasia (blue arrow) and extensive inflammatory cellular infiltrate (*). (G) Shows severe intra-alveolar inflammatory infiltrate. (H) Shows numerous intra alveolar foamy macrophages (thick arrow). (I-J) LBP +Ti group. (I) Shows few collapsed alveoli (A1) among normal ones (A2), less thick interalveolar septa (arrow head), less congestion (V), normal bronchioles (B1), disfigured bronchioles (B2). (J) Shows a bronchiole with areas of epithelial hyperplasia (blue arrow) alternating with epithelial desquamation (black arrow), minimal peribronchiolar inflammatory infiltrate (*). (K-N) LBP + Ti + ZnPPIX group. (K) Shows broncho-vascular bundle (B) & (V) with severe congestion, granuloma (*). (L) Shows collapsed air spaces (A), markedly thick interalveolar septa (arrow). (M) Shows a granuloma (G) damaging alveolar walls and obstructing alveolar lumen. (N) Shows abundant intra-alveolar macrophages (thick arrow). H&E ×100 (A, C, E, I, K); × 400 (B, D, F, G, H, J, L, M, N). NC: normal control group; LBP: *Lycium barbarum polysaccharide*; Ti: TiO_2NPs; ZnPPIX: Zinc protoporphyrin IX.

Figure 9 (G-K)), all displayed a positive brownish reaction. This reaction appeared minimal and limited to few cells in control and LBP groups but became significantly stronger and widely distributed in Ti group relative to the control one. Fortunately, LBP pretreatment induced a noticeable improvement manifested as a significant decline in the immune-histochemical reaction comparable to Ti group. Yet, co-administration of ZnPPIX elicited a substantial enhancement in the immune reaction when contrasted with LPB+ Ti group. These findings were further statistically established by quantification of the mean area percentage of caspase3, NF-κB and TLR4 immuno-expression (Figure 6 (F)-(L); Figure 8 (F)-(L); Figure 9 (F)-(L)). Further, the mean number of CD68 immune +ve macrophages/high power field (×400) was calculated (Figure 7 F, L).

Discussion

TiO_2 NPs triggers oxidative stress and inflammatory reaction.[32-34] In our study, the histological insults observed due to TiO_2 NPs exposure align with the findings of Suker & Jasim[35] who attributed them to excessive ROS production. Overproduction of ROS disrupts the cell cycle, leading to apoptosis and inflammation in intestinal and hepatic tissues.[36] The current study stated that LBP reduced TiO_2 NPs induced detrimental changes. In the same context, LBP mitigated skin cell cytotoxicity, improved cellular morphology, reduced intracellular ROS levels and decreased cell apoptosis.[37] In the present study, LBP mitigated oxidative stress and even boosted the activity of antioxidant defense enzymes. These findings are consistent with Zheng *et al.*[24] who attributed LBP benefits to the ability to activate Nrf2 and its downstream effecter, HO-1 which coincides with the present study. LBP provides protection

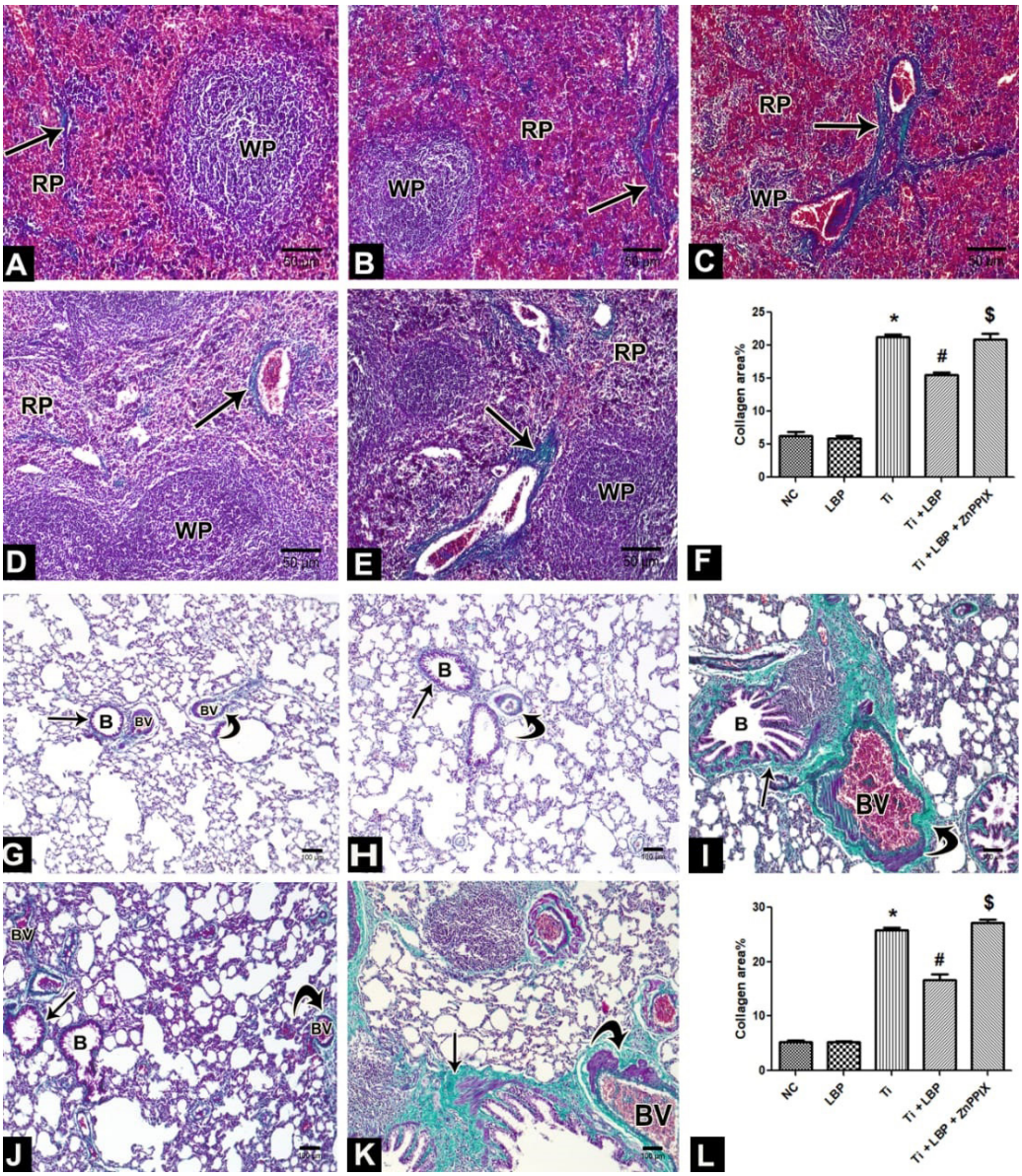

Figure 5. Photomicrographs of MT stained spleen (A-E) and lung (G-K) sections showing green colored collagen deposit around splenic vessels (arrow), pulmonary vessels (curved arrow) and bronchioles (small arrow). The collagen amount appears little and finely distributed in both NC and LBP groups in the spleen (A-B) and lung (G-H). Ti group: collagen deposit is dense and widely distributed in both spleen (C) and lung (I). LBP+ Ti group: less collagen deposition in both spleen (D) and lung (J). LBP + Ti +ZnPPIX group: an abundant collagen deposit in both spleen (E) and lung (K) (MT×100). Bar charts (F) - (L). Morphometric analysis of MT area % mean values in spleen (F) and lung (L). NC: normal control group; LBP: *Lycium barbarum polysaccharide*; Ti: TiO_2NPs; ZnPPIX: Zinc protoporphyrin IX. Values are presented as means ± SD. * $p < 0.05$ significant vs. NC group, $^{\#}$ $p < 0.05$ significant vs. Ti group, $^{\$}$ $p < 0.05$ significant vs. LBP+ Ti group.

to the skin against ultraviolet B (UVB) irradiation by activating Nrf2 / HO-1 signaling cascades, scavenging free radicals, and preventing DNA destruction.[38] LBP reduces oxidative reactions and enhances cell adaptive antioxidant pathways in the retina of rodents suffering from ischemia-reperfusion insult.[39] Furthermore, it has been reported that detoxifying enzymes and radical scavengers, dependent on the antioxidant response element (ARE), are essential components against oxidative tissue destruction and for maintaining cell homeostasis.[40] The detoxifying enzymes HO-1, SOD, and CAT are encoded by Nrf2.[41] Upon exposure to either ROS or pharmacological ligands, Nrf2 dissociates from the Keap-1 protein and enters the nucleus to induce the transcription of antioxidant enzymes (SOD, CAT, and HO-1) through ARE.[42] In the present study, TiO_2NPs induced spleen insults coincide with other established animal reports.[43,44] Additionally, caspase-3 can be activated by both intrinsic and extrinsic apoptotic pathways, causing DNA damage.[45] TiO_2 NPs induce cell apoptosis by upregulating apoptotic cellular elements.[46] TiO_2 NPs target the mitochondrial intrinsic apoptotic pathway and stimulate cytochrome C surge into the cytosol causing caspase 3 activation. The active pro-apoptotic protein, Bax, via micropores formation in the mitochondrial membrane causes protein leakage into the cytosol. Herein, Bcl2, as a regulator for apoptosis, prevents

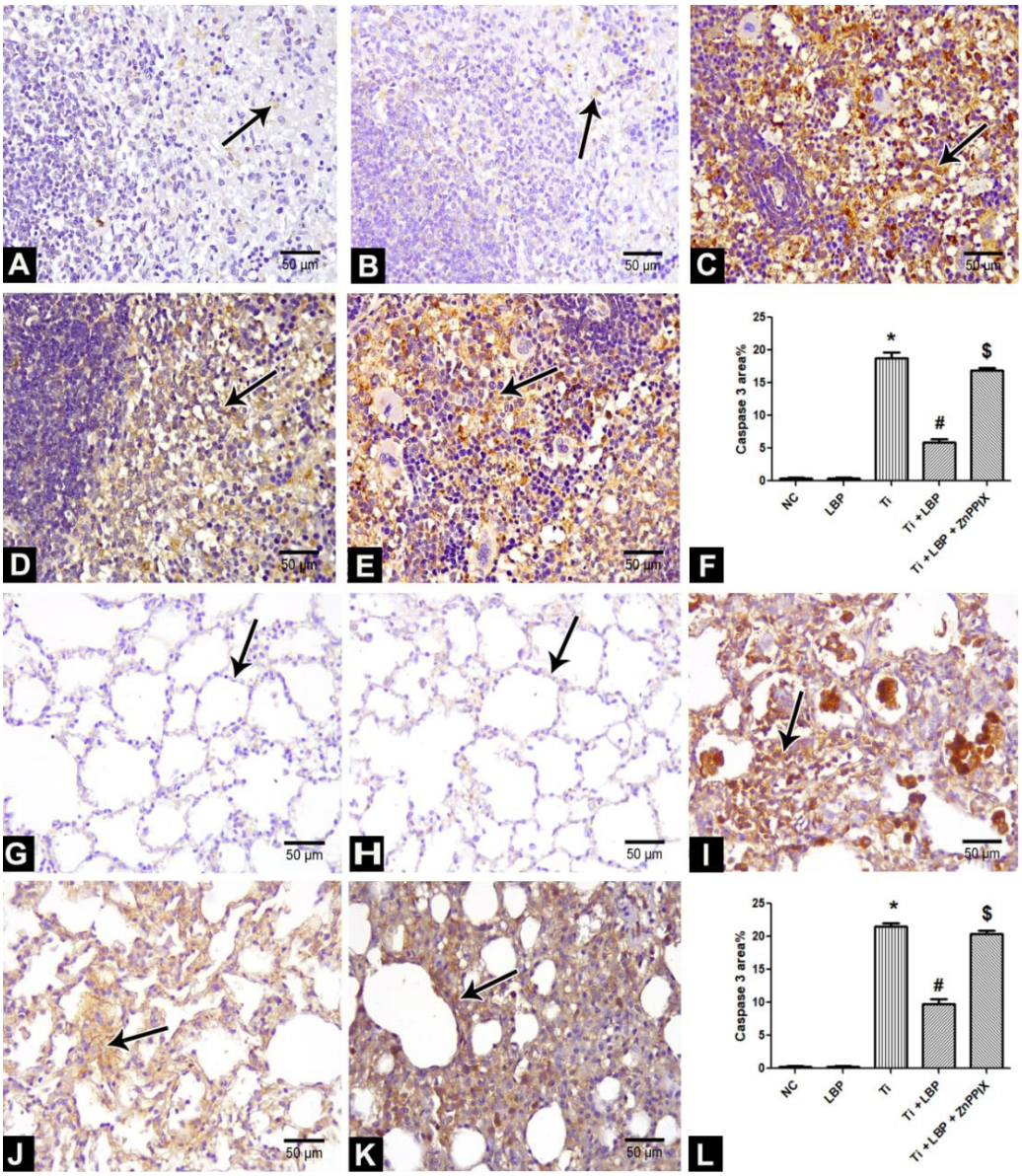

Figure 6. Photomicrographs of immunohistochemically stained spleen (A-E) and lung (G-K) sections labeled with anti-caspase-3 antibody showing brownish cytoplasmic reaction (arrow). The reaction is minimal and limited to few cells in Control and LBP groups in the spleen (A-B) and lung (G-H). Ti group: the reaction is strong and widely distributed in spleen (C) and lung (I). LBP+ Ti group: minimal limited reaction in the spleen (D) and lung (J). LBP + Ti + ZnPPIX group: strong widely distributed reaction in spleen (E) and lung (K) (Caspase 3 immunostaining×400). Bar charts (F) - (L). Morphometric analysis of Caspase 3 area % mean values in the spleen (F) and lung (L). NC: normal control group; LBP: *Lycium barbarum polysaccharide*; Ti: TiO_2 NPs; ZnPPIX: Zinc protoporphyrin IX. Values are presented as means ± SD. * $p < 0.05$ significant vs. NC group, $^{\#}$ $p < 0.05$ significant vs. Ti group. $^{\$}$ $p < 0.05$ significant vs. LBP +.Ti group.

cytochrome C release to stop caspase 3 activation.[47,48] The current results suggested the involvement of HO-1 in the anti-apoptotic effect of LBP. In agreement with our suggestion, Luo *et al.*[49] reported that HO-1exerts a valuable role in preventing cell apoptosis either directly or by interfering with ROS generation. Additionally, heme breaks down into carbon monoxide (CO), iron, and biliverdin / bilirubin with the help of HO-1, endowing HO-1 with the merit of being an inspiring antioxidant, anti-inflammatory and anti-apoptotic cellular factor.[13] A previous report showed that, LBP induced a significant upregulation of Nrf2 / HO-1 expression as well as the antioxidant and anti-apoptotic effects of LBP were counteracted by either HO-1 suppression or Nrf2 silencing.[28] The current work align with previous studies[50-54] which demonstrated that exposure to TiO_2 NPs upregulated the expression of numerous inflammatory cytokines and chemokines, all of which act as chemoattractant for leukocytes and other cells involved in the inflammatory response. Giribabu *et al.*[55] asserted that NF-κB-mediated macrophage recruitment, extracellular matrix deposition, fibrosis, and ultimately renal architecture devastation. Moreover, Qi *et al.*[56] reported that LBP reduced the gene and protein expression of TLR4, MyD88, and NF-κB, thereby exerting protective actions against inflammation in type-2 diabetic mice. The incorporation of HO-1 enhancement and TLR4

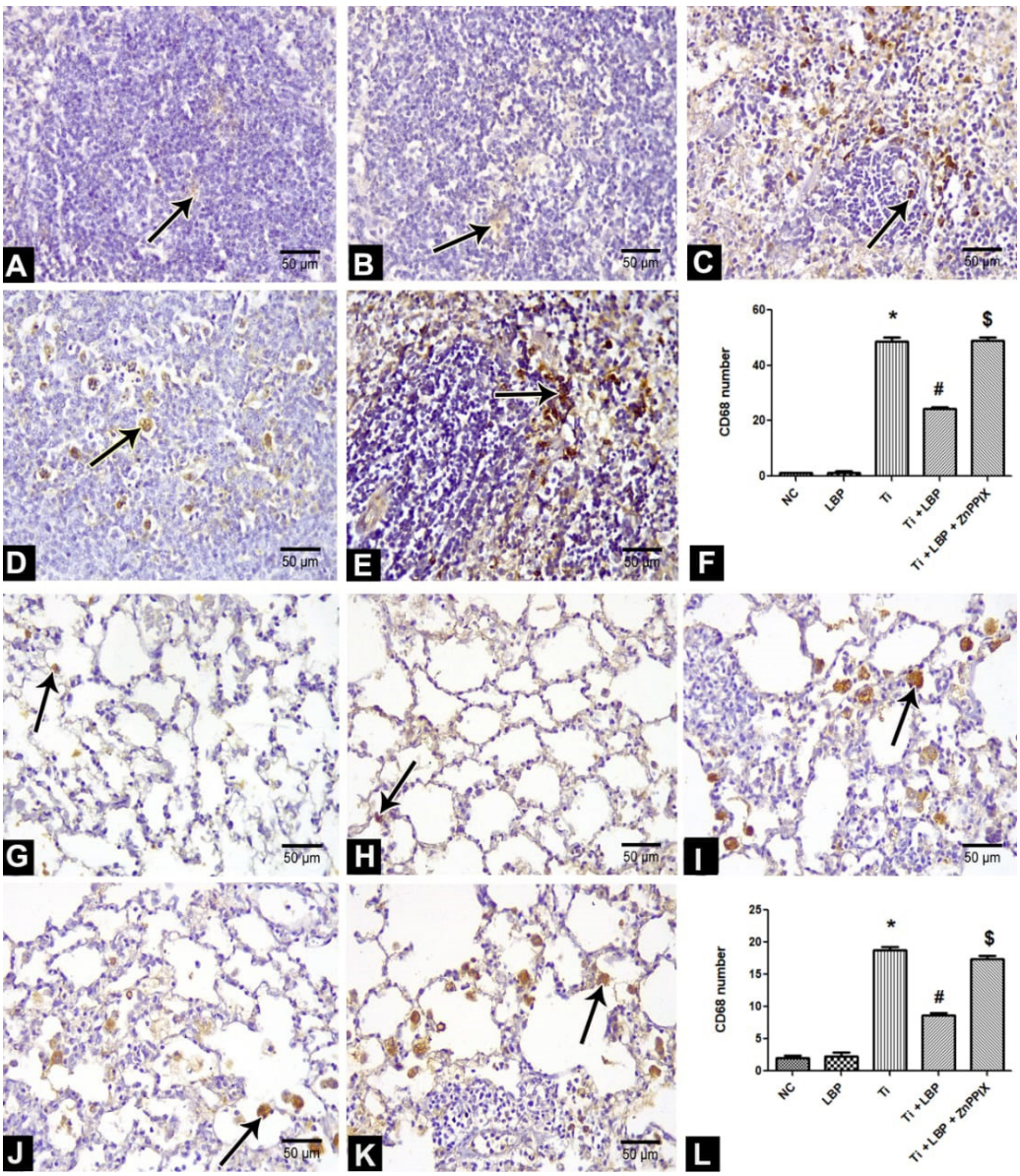

Figure 7. Photomicrographs of immunohistochemically stained spleen (A-E) and lung (G-K) sections labeled with anti-CD68 antibody showing brownish colored immuno-positive macrophages (arrow).The reaction is limited to few macrophages in Control and LBP groups in the spleen (A-B) and lung (G-H). TiO_2 NPs group: shows marked increase in the number of immuno-positive macrophages in the spleen (C) and lung (I). LBP + Ti group: marked reduction in CD68 +ve cell number in the spleen (D) and lung (J). LBP+ Ti +ZnPPIX group: marked increase in number of immuno-positive macrophages in the spleen (E) and lung (K). (CD68 immunostaining ×400). Bar charts (F) - (L). Morphometric analysis of the mean number of immuno-positive macrophages in the spleen (F) and lung (L). NC: normal control group; LBP: *Lycium barbarum polysaccharide;* Ti: TiO_2NPs; ZnPPIX: Zinc protoporphyrin IX. Values are presented as means ± SD. * $p < 0.05$ significant vs. NC group, $^{\#}$ $p < 0.05$ significant vs. Ti group, $^{\$}$ $p < 0.05$ significant vs. LBP+ Ti group.

signaling was suggested by Shen *et al.*[19], who found that HO-1 induced by copper modulated TLR4 signaling and mitigated liver damage in a model of ischemia-reperfusion in mice. This indicates a cross-relationship between HO-1 signaling and the TLR4 pathway. The crosstalk between HO-1 and the TLR4/MyD88/NF-κB pathway is vital for regulating inflammation. While HO-1 modulates oxidative stress, TLR4 modulates the adaptive immune response, as noted by Mohan and Gupta.[57] Furthermore, HO-1 and its upstream regulator, Nrf2, were found to reduce the inflammatory response mediated by TLR4l.[58] In the present work, extramedullary hematopoiesis was mediated by TiO_2 NPs which was also reported in response to various metallic NPs.[59] Recent research by Jin *et al.*[60] proposed that, excess megakaryocytes may lead to increased platelet synthesis, and thus increase the risk of thromboembolic incidence. LBP restored megakaryocyte density in the red pulp. The immunomodulatory and anti-inflammatory characteristics of LBP may be responsible for this. Nevertheless, more research is needed to determine the precise mechanism. The spleen and lung fibrosis produced by TiO_2 NPs aligns with the findings from prior research.[61] Previous studies have suggested that inflammatory cells migrate to and proliferate at damaged sites, releasing various cytokines that can further recruit cells and remodel the matrix, resulting in excessive production of collagen and matrix

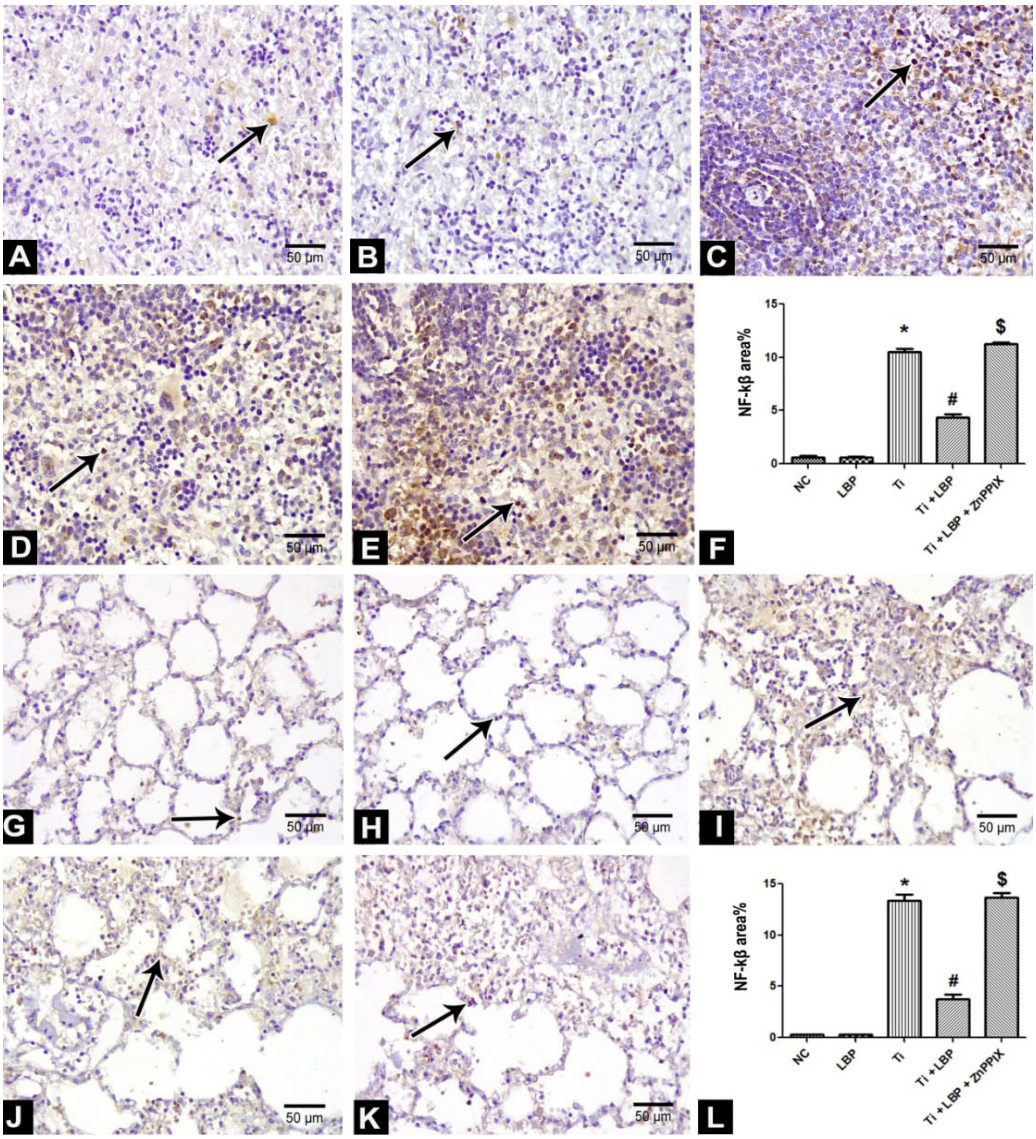

Figure 8. Photomicrographs of immunohistochemically stained spleen (A-E) and lung (G-K) sections labeled with anti- NF-κB antibody showing brownish nuclear reaction (arrow). The reaction is minimal and limited to few cells in NC and LBP groups in the spleen (A-B) and lung (G-H). Ti group: the reaction is extensive involving a great number of cells in both spleen (C) and lung (I). LBP+ Ti group: minimal limited reaction in the spleen (D) and lung (J). LBP + Ti +ZnPPIX group: extensive widely distributed reaction in both spleen (E) and lung (K) (NF-κB immunostaining ×400). Bar charts (F)- (L). Morphometric analysis of NF-κB area % mean values in the spleen (F) and lung (L). NC: normal control group; LBP: *Lycium barbarum polysaccharide*; Ti: TiO_2NPs; ZnPPIX: Zinc protoporphyrin IX. Values are presented as means ± SD. * $p < 0.05$ significant vs. NC group, $^{\#}$ $p < 0.05$ significant vs. Ti group, $^{\$}$ $p < 0.05$ significant vs. LBP+ Ti group.

components.[62] In addition, LBP demonstrated anti-fibrotic properties against TiO_2 NPs. Consistent with our findings, Xiao *et al.*[63] reported that LBP has a hepatoprotective effect against non-alcoholic steatohepatitis in rats by inhibiting the TGF-β1 signaling pathway. Moreover, NF-κB has been implicated in promoting the production of numerous inflammatory cytokines, especially TGF-β1, leading to increased proliferation of fibroblasts and macrophages, ultimately causing enhanced collagen deposition.[64] Moreover, the stimulation of TLR-4 signaling in fibroblasts has been linked to increased collagen deposition and elevated expression of genes involved in tissue repair and the extracellular matrix.[65] In a related context, Seki *et al.*[66] found that the modulation of TGF-β1 signaling in a mouse model of liver fibrosis is dependent on the TLR4 / MyD88 / NF-κB axis. Therefore, a link between proinflammatory and profibrogenic pathways was established, a correlation that aligns with the findings of the present work.

Conclusion

Acute exposure to TiO_2 NPs induces well defined biochemical and histological detrimental effects on spleen and lung affecting their functions. The toxicity induced by TiO_2 NPs is likely linked to the induction of oxidative stress, inflammation, apoptosis, and fibrosis. Additionally, the amelioration of TiO_2 NPs-induced toxicity by LBP is attributed to the activation of HO-1, along with the modulation of TGF-β1 and the TLR4/NF-κB signaling pathway.

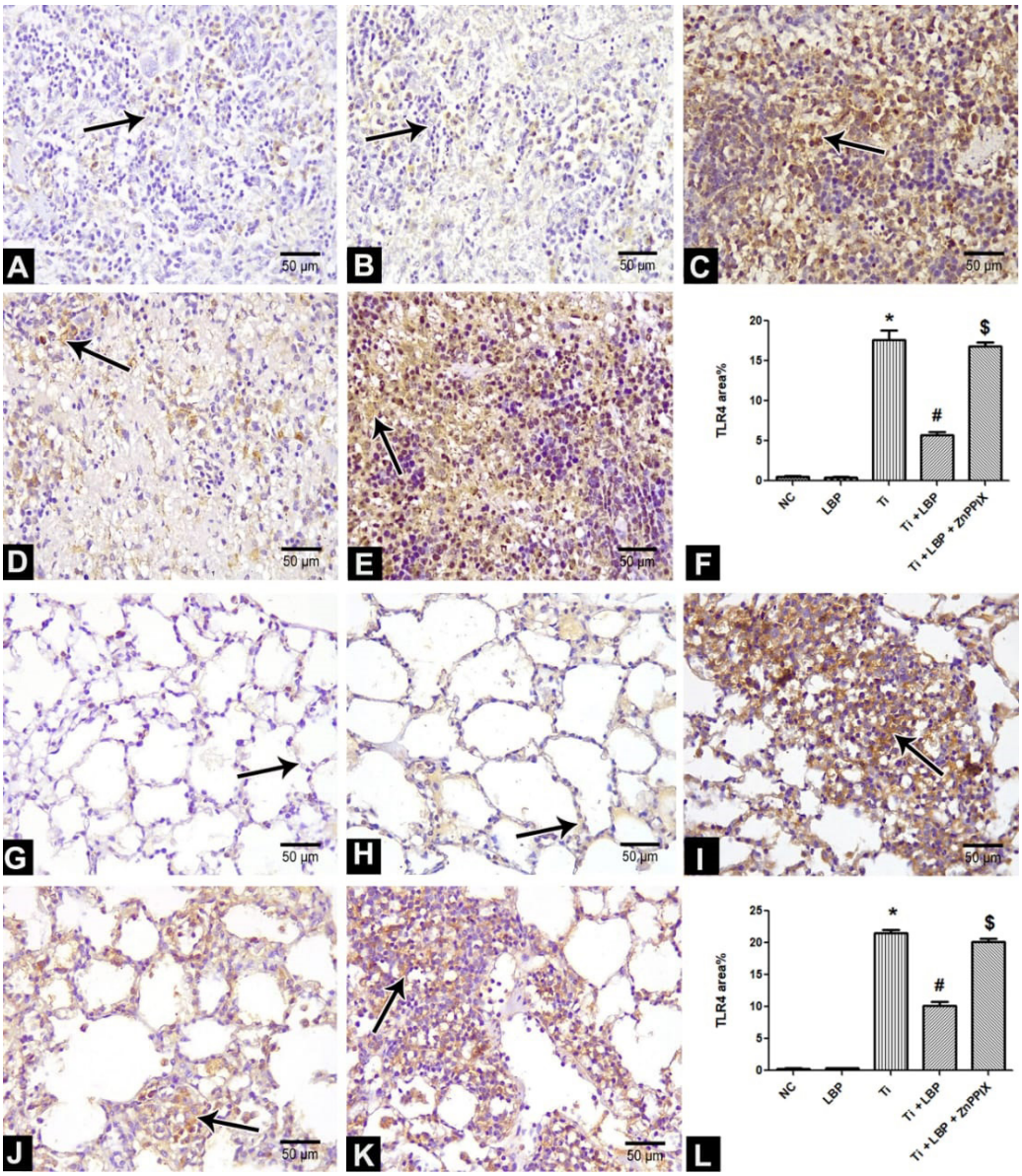

Figure 9. Photomicrographs of immunohistochemically stained spleen (A-E) and lung (G-K) sections labeled with anti-TLR4 antibody showing brownish reaction (arrow). The reaction is minimal and limited to few cells in Control and LBP groups in the spleen (A-B) and lung (G-H). Ti group: the reaction is extensive involving a great number of cells in both spleen (C) and lung (I). LBP+ Ti group: shows minimal limited reaction in the spleen (D) and lung (J). LBP + Ti +ZnPPIX group: shows extensive widely distributed reaction in both spleen (E) and lung (K) (TLR4 immunostaining ×400). Bar charts (F) - (L). Morphometric analysis of TLR4 area % mean values in the spleen (F) and lung (L). NC: normal control group; LBP: *Lycium barbarum polysaccharide*; Ti: TiO_2NPs; ZnPPIX: Zinc protoporphyrin IX. Values are presented as means ± SD. * $p < 0.05$ significant vs. NC group, # $p < 0.05$ significant vs. Ti group, $ $p < 0.05$ significant vs. LBP+ Ti group.

Ethical Issues

Laboratory animal guidelines for care and use were followed in the protocol of our study. Also, the protocol was approved by the Institutional Animal Care and Use Committee [IACUC], Zagazig University (ZU), with a reference number (ZU-IACUC/3/F/202/2023).

Author Contributions

Amal S. Sewelam: Methodology, Investigation, Writing – Review & Editing. Soad L. Kabil: Conceptualization, Methodology, Formal Analysis, Writing – Original Draft. Bashir Jarrar: Writing- Review & Editing. Mohamed Ahmed Sabry: Methodology, Writing – Review & Editing. Manal Mohammed Morsy: Formal Analysis, Writing – Review & Editing

Conflict of Interest

The authors declared no potential conflicts of interest with respect to the research, authorship, and/or publication of this article.

References

1. Verma V, Al-Dossari M, Singh J, Rawat M, Kordy MGM, Shaban M. A Review on green synthesis of TiO_2 NPs: Photocatalysis and antimicrobial applications. Polymers (Basel). 2022;14(7):1444. doi:10.3390/polym14071444

2. Irshad MA, Nawaz R, Rehman MZU, Adrees M, Rizwan M, Ali S, et al . Synthesis, characterization and advanced sustainable applications of titanium dioxide nanoparticles: A review. Ecotoxicol Environ Saf. 2021;212:111978. doi:10.1016 / j.ecoenv.2021.111978
3. Ziental D, Czarczynska-Goslinska B, Mlynarczyk DT, Glowacka-Sobotta A, Stanisz B, Goslinski T et al. Titanium dioxide nanoparticles: prospects and applications in medicine. Nanomaterials (Basel). 2020;10(2):387. doi:10.3390 / nano10020387
4. Shakeel M, Jabeen F, Shabbir S, Asghar MS, Khan MS, Chaudhry AS. Toxicity of Nano-Titanium Dioxide (TiO_2-NP) Through Various Routes of Exposure: a Review. Biol Trace Elem Res. 2016;172(1):1-36. doi:10.1007/s12011-015-0550-x
5. Kumah EA, Fopa RD, Harati S, Boadu P, Zohoori FV, Pak T. Human and environmental impacts of nanoparticles: a scoping review of the current literature. BMC Public Health. 2023;23(1):1059. doi:10.1186/s12889-023-15958-4
6. Dar GI, Saeed M, Wu A. Toxicity of TiO2 nanoparticles. In: Wu A, Ren W, editors. TiO2 nanoparticles: Applications in nanobiotechnology and nanomedicine. Hoboken: Wiley; 2020. doi:10.1002/9783527825431.ch2
7. Mohammadparast V, Mallard BL. The effect and underlying mechanisms of titanium dioxide nanoparticles on glucose homeostasis: A literature review. J Appl Toxicol. 2023;43(1):22-31. doi:10.1002/jat.4318
8. Chen J, Dong X, Zhao J, Tang G. In vivo acute toxicity of titanium dioxide nanoparticles to mice after intraperitioneal injection. J Appl Toxicol. 2009;29(4):330-7. doi:10.1002/jat.1414
9. Zhang R, Niu Y, Li Y, Zheo C, Song B. Li Y, et al. Acute toxicity study of the interaction between titanium dioxide nanoparticles and lead acetate in mice. Environ Toxicol Pharmacolo. 2010;30 (1):52-60. doi:10.1016/j.etap.2010.03.015
10. Cataldi M, Vigliotti C, Mosca T, Cammarota MR, Capone D. Emerging Role of the Spleen in the Pharmacokinetics of Monoclonal Antibodies, Nanoparticles and Exosomes. Int J Mol Sci. 2017;18(6):1249. doi:10.3390/ijms18061249
11. Rashid MM, Forte Tavčer P, Tomšič B. Influence of titanium dioxide nanoparticles on human health and the environment. Nanomaterials (Basel). 2021;11(9):2354. doi:10.3390/nano11092354
12. Liu JJ, Zhao GX, He LL, Wang Z, Zibrila AI, Niu B, et al. *Lycium barbarum* polysaccharides inhibit ischemia/reperfusion-induced myocardial injury via the Nrf2 antioxidant pathway. Toxicol Rep. 2021;8:657-667. doi:10.1016/j.toxrep.2021.03.019
13. Ryter SW. Heme Oxygenase-1: An anti-inflammatory effecter in cardiovascular, lung, and related metabolic disorders. Antioxidants (Basel). 2022;11(3): 555. doi:10.3390/antiox11030555
14. Nowis D, Bugajski M, Winiarska M, Bil J, Szokalska A, Salwa P, et al. Zinc protoporphyrin IX, a heme oxygenase-1 inhibitor, demonstrates potent antitumor effects but is unable to potentiate antitumor effects of chemotherapeutics in mice. BMC Cancer. 2008;8:197. doi:10.1186/1471-2407-8-197
15. Zhang S, Feng Z, Gao W, Duan Y, Fan G., Geng X, et al. Aucubin Attenuates liver ischemia-reperfusion injury by inhibiting the HMGB1/TLR-4/NF-κB signaling pathway, oxidative stress, and apoptosis. Front Pharmacol. 2020;11:544124. doi:10.3389/fphar.2020.544124
16. Li X, Yao Q, Huang J, Jin Q, Xu B, Chen F, et al. Morin hydrate inhibits TREM-1/TLR4-mediated inflammatory response in macrophages and protects against carbon tetrachloride-induced acute liver injury in mice. Front Pharmacol. 2019;10:1089. doi:10.3389/fphar.2019.01089
17. Jiang A, Zhang Y, Zhang X, Wu D, Liu Z, Li S, et al. Morin alleviates LPS-induced mastitis by inhibiting the PI3K/AKT, MAPK, NF-κB and NLRP3 signaling pathway and protecting the integrity of blood-milk barrier. Int Immunopharmacol. 2020;78:105972. doi:10.1016/j.intimp.2019.105972
18. Zheng C, Chen J, Chu F, Zhu J, Jin T. Inflammatory role of TLR-MyD88 signaling in multiple sclerosis. Front Mol Neurosci. 2020;12:314. doi:10.3389/fnmol.2019.00314
19. Shen XD, Ke B, Zhai Y, Gao F, Busuttil RW, Cheng G, et al. Toll-like receptor and heme oxygenase-1 signaling in hepatic ischemia/reperfusion injury. Am J Transplant. 2005;5(8):1793-800. doi:10.1111/j.1600-6143.2005.00932.x
20. Chen L, Li W, Qi D, Wang D. *Lycium barbarum* polysaccharide protects against LPS-induced ARDS by inhibiting apoptosis, oxidative stress, and inflammation in pulmonary endothelial cells. Free Radic Res. 2018;52(4):480-90. doi:10.1080/10715762.2018.1447105
21. Hong CY, Zhang HD, Liu XY, Xu Y. Attenuation of hyperoxic acute lung injury by *Lycium barbarum* polysaccharide via inhibiting NLRP3 inflammasome. Arch Pharm Res. 2019;42(10):902-908. doi:10.1007/s12272-019-01175-4
22. Bo R, Liu Z, Zhang J, Gu P, Ou N, Sun Y, et al. Mechanism of *Lycium barbarum* polysaccharides liposomes on activating murine dendritic cells. Carbohydr Polym. 2019;205:540-9. doi:10.1016/j.carbpol.2018.10.057
23. Xiao Z, Deng Q, Zhou W, Zhang Y. Immune activities of polysaccharides isolated from Lycium barbarum L. What do we know so far? Pharmacol Ther. 2022;229:107921. doi:10.1016/j.pharm thera.2021.107921
24. Zheng G, Ren H, Li H, Li X, Dong T, Xu S, et al. *Lycium barbarum* polysaccharide reduces hyperoxic acute lung injury in mice through Nrf2 pathway. Biomed Pharmacother. 2019;111:733-39. doi:10.1016/j.biopha.2018.12.073

25. Zheng X, Wang J, Bi F, Li Y, Xiao J, Chai Z et al. Protective effects of *Lycium barbarum* polysaccharide on ovariectomy - induced cognition reduction in aging mice. Int J Mol Med. 2021;48(1):121. doi:10.3892/ijmm.2021.4954
26. Kwok SS, Wong FS, Shih KC, Chan Y, Bu Y, Chan TC et al. *Lycium barbarum* polysaccharide suppresses expression of fibrotic proteins in primary human corneal fibroblasts. J Clin Med. 2020;9(11):3572. doi:10.3390/jcm9113572
27. Al- Doaiss A, Jarrar B, Shati A, Al-Kahtani M, Alfaifi M. Cardiac and testicular alterations induced by acute exposure to titanium dioxide nanoparticles: Histopathological study. IET Nanobiotechnol. 2021;15:58-67. doi:10.1049/nbt2.12000
28. Cao S, Du J, Hei Q. *Lycium barbarum* polysaccharide protects against neurotoxicity via the Nrf2-HO-1 pathway. Exp Ther Med. 2017;14 (5):4919-27. doi:10.3892/etm.2017.5127
29. Suvarna KS, Layton C, Bancroft JD. Bancroft's theory and techniques of histological practice. Amsterdam: Elsevier; 2019. doi:10.1016/C2015-0-00143-5
30. Torlakovic EE, Nielsen S, Vyberg M, Taylor CR. Getting controls under control: the time is now for immunohistochemistry. J Clin Pathol. 2015;68:879-82. doi:10.1136/jclinpath-2014-202705
31. Alsemeh AE, Hulail MAE, Mokhtar HEL, Eldemerdash RT, Banatean-Dunea I, Fericean LM, et al. Tempol improves optic nerve histopathology and ultrastructures in cisplatin-induced optic neuropathy in rats by targeting oxidative stress-endoplasmic reticulum stress-autophagy signaling pathways. Front Cell Neurosci. 2023;17:1256299. doi:10.3389/fncel.2023.1256299
32. Jia X, Wang S, Zhou L, Sun L. The Potential Liver, Brain, and embryo toxicity of titanium dioxide nanoparticles on mice. Nanoscale Res Lett. 2017;12(1):478. doi:10.1186/s11671-017-2242-2
33. Li C, Tang M. The toxicological effects of nano titanium dioxide on target organs and mechanisms of toxicity. J Appl Toxicol. 2024;44(2):152-64. doi:10.1002/jat.4534
34. Valentini X, Rugira P, Frau A, Tagliatti V, Conotte R, Laurent S, et al. Hepatic and renal toxicity induced by TiO_2 nanoparticles in rats: A morphological and metabonomic study. J Toxicol. 2019;3:5767012. doi:10.1155/2019/5767012
35. Suker DK, Jasim FA. Liver histopathological alteration after repeated intra-tracheal instillation of titanium dioxide in male rats. Gastroenterol Hepatol Bed Bench. 2018;11(2):159-68.
36. Abbasi-Oshaghi E, Mirzaei F, Pourjafar M. NLRP3 inflammasome, oxidative stress, and apoptosis induced in the intestine and liver of rats treated with titanium dioxide nanoparticles: in vivo and in vitro study. Int J Nanomedicine. 2019;14:1919-36. doi:10.2147/ IJN. S192382
37. Zhu S, Li X, Dang B, Wu F, Wang C, Lin C. *Lycium barbarum* polysaccharide protects HaCa T cells from PM 2.5-induced apoptosis via inhibiting oxidative stress, ER stress and autophagy. Redox Rep. 2022;27(1):32-44. doi:10.1080/13510002.2022.2036507
38. Qi B, Ji Q, Wen Y, Liu L, Guo X, Hou G, et al. *Lycium barbarum* polysaccharides protect human lens epithelial cells against oxidative stress-induced apoptosis and senescence. PLoS One. 2014;9(10):e110275. doi:10.1371/journal.pone.0110275
39. He M, Pan H, Chang RC, So K, Brecha NC, Pu M. Activation of the Nrf2/HO-1 antioxidant pathway contributes to the protective effects of *Lycium barbarum* polysaccharides in the rodent retina after ischemia-reperfusion-induced damage. PLoS One. 2014;9(1):e84800. doi:10.1371/ journal.pone.0084800
40. Gao Y, Wei Y, Wang Y, Gao F, Chen Z. *Lycium barbarum*: A traditional chinese herb and a promising anti-aging agent. Aging Dis. 2017;8(6):778-91. doi:10.14336/AD.2017.0725
41. Yi S, Chen S, Xiang J, Tan J, Huang K, Zhang H, et al. Genistein exerts a cell-protective effect via Nrf2/HO-1/PI3K signaling in Ab25-35-induced Alzheimer's disease models in vitro. Folia Histochem Cytobiol. 2021;59(1):49-56. doi:10.5603/FHC.a2021.0006
42. Bai Z, Wang Z. Genistein protects against doxorubicin-induced cardiotoxicity through Nrf-2 / HO-1 signaling in mice model. Environ Toxicol. 2019;34(5):645-51. doi:10.1002/tox.22730
43. Korani M, Rezayat SM, Gilani K, Bidgoli SA, Adeli S. Acute and subchronic dermal toxicity of nanosilver in guinea pig. Int J Nanomedicine. 2011;6:855-62. doi:10.214 /IJN. S17065
44. Abass MA, Selim SA, Selim AO, El-Shal A, Gouda ZA. Effect of orally administered zinc oxide nanoparticles on albino rat thymus and spleen. IUBMB Life. 2017;69(7):528-39. doi:10.1002/iub.1638
45. Abdel-Halim KY, Osman SR, Abuzeid MAF, El-Danasoury HTM, Khozimy AM. Apoptotic and histopathological defects enhanced by titanium dioxide nanoparticles in male mice after short-term exposure. Toxicol Rep. 2022;9:1331-46. doi:10.1016/j.toxrep.2022.06.003
46. Gholinejad Z, Ansari MHK, Rasmi Y. Titanium dioxide nanoparticles induce endothelial cell apoptosis via cell membrane oxidative damage and p38, PI3K / Akt, NF-κB signaling pathways modulation. J Trace Elem Med Biol. 2019;54:27-35. doi:10.1016/j.jtemb.2019.03.008
47. Duan SM, Zhang YL, Wang Y. Effects of titanium dioxide nanoparticles and lipopolysaccharide on antioxidant function of liver tissues in mice. Beijing Da Xue Xue Bao Yi Xue Ban. 2018;50(3):395-400.
48. Urbani A, Prosdocimi E, Carrer A, Checchetto V, Szabo I. Mitochondrial ion channels of the inner membrane and their regulation in cell death signaling. Front Cell Dev Biol. 2021;8:620081. doi:10.3389/fcell.2020.620081
49. Luo C, Chen H, Wang Y, Lin G, Li C, Tan L, et al. Protective effect of coptisine free base on indomethacin-

induced gastric ulcers in rats: Characterization of potential molecular mechanisms. Life Sci. 2018;193:47-56. doi:10.1016/j.lfs.2017.12.004

50. Hong F, Yu X, Wu N, Zhang YQ. Progress of in vivo studies on the systemic toxicities induced by titanium dioxide nanoparticles. Toxicol Res (Camb). 2017;6(2):115-33. doi:10.1039/c6tx00338a
51. Mikusova ML, Busova M, Tulinska J, Masanova V, Liskova A, Uhnakoya I, et al. Titanium dioxide nanoparticles modulate systemic immune response and increase levels of reduced glutathione in mice after seven-week inhalation. Nanomaterials (Basel). 2023;13(4):767. doi:10.3390/nano13040767
52. Kumar S, Meena R, Paulraj R. Role of macrophage (M1 and M2) in titanium-dioxide nanoparticle-induced oxidative stress and inflammatory response in rat. Appl Bio Biotechnol. 2016;180(7):1257-75. doi:10.1007/s12010-016-2165-x
53. Mohammed ET, Safwat GM. Grape seed proanthocyanidin extract mitigates titanium dioxide nanoparticle (TiO_2-NPs)-induced hepatotoxicity through TLR-4 / NF-κB signaling pathway. Biol Trace Elem Res. 2020;196(2):579-89. doi:10.1007/s12011-019-01955-5
54. Pugazhendhi A, Prabhu R, Muruganantham K, Shanmuganathan R, Natarajan S. Anticancer, antimicrobial and photocatalytic activities of green synthesized magnesium oxide nanoparticles (MgO NPs) using aqueous extract of *Sargassum wightii*. J Photochem Photobiol B. 2019;190:86-97. doi:10.1016/j.jphotobiol. 2018.11.014
55. Giribabu N, Karim K, Kilari EK, Salleh N. *Phyllanthus niruri* leaves aqueous extract improves kidney functions, ameliorates kidney oxidative stress, inflammation, fibrosis and apoptosis and enhances kidney cell proliferation in adult male rats with diabetes mellitus. J Ethnopharmacol. 2017;205:123-137. doi:10.1016/j.jep.2017.05.002
56. Qi Y, Duan G, Fan G, Peng N. Effect of *Lycium barbarum* polysaccharides on cell signal transduction pathways. Biomed Pharmacother. 2022;147:112620. doi:10.1016/j.biopha.2022.112620
57. Mohan S, Gupta D. Crosstalk of toll-like receptors signaling and Nrf2 pathway for regulation of inflammation. Biomed Pharmacother. 2018;108:1866-78. doi:10.1016/j.biopha.2018.10.019
58. Chen JY, Zhu GY, Su XH, Wan R, Liu J, Liao K et al. 7-deacetylgedunin suppresses inflammatory responses through activation of Keap1/Nrf2/HO-1 signaling. Oncotarget. 2017;8(33):55051-63. doi:10.18632/oncotarget.19017
59. Mazen NF, Saleh EZ, Mahmoud AA, Shaalan A. Histological and immunohistochemical study on the potential toxicity of sliver nanoparticles on the structure of the spleen in adult male albino rats. Egypt J Histol. 2017;40 (3):374-87. doi:10.21608/EJH.2017.4662
60. Jin X, Zhang Z, Guan G, Zhou Q, Zheng Y, Jiang G. Silica nanoparticles promote the megakaryocyte maturation and differentiation: Potential implications for hematological homeostasis. ACS Appl Mater Interfaces. 2023;15 (25):29948-57. doi:10.1021/acsami.3c04046
61. Hong F, Ji J, Ze X, Zhoue Y, Ze Y. Liver inflammation and fibrosis induced by long-term exposure to nano titanium dioxide (TiO_2) nanoparticles in mice and its molecular mechanism. J Biomed Nanotechnol. 2020;16(5):616-25. doi:10.1166 / jbn.2020.2921
62. .Fanny M, Nascimento M, Baron L, Schricke C, Maillet I, Akbal M, et al. The IL-33 receptor ST2 regulates pulmonary inflammation and fibrosis to bleomycin. Front Immunol. 2018;9:1476. doi:10.3389/fimmu.2018.01476
63. Xiao J, Liong EC, Ching YP, Chang RCC, Fung ML, Xu AM, et al. *Lycium barbarum* polysaccharides protect rat liver from non-alcoholic steatohepatitis-induced injury. Nutr Diabetes. 2013;3(7):e81. doi:10.1038/nutd.2013.22
64. Comeglio P, Filippi S, Sarchielli E, Morelli A, Cellai I, Corno C, et al. Therapeutic effects of obeticholic acid (OCA) treatment in a bleomycin-induced pulmonary fibrosis rat model. J Endocrinol Invest. 2019;42(3):283-294. doi:10.1007/s40618-018-0913-1
65. Bhattacharyya S, Wang W, Qin W, Cheng K, Coulup S, Chavez S, et al. TLR4-dependent fibroblast activation drives persistent organ fibrosis in skin and lung. JCI Insight. 2018;3(13):e98850. doi:10.1172/jci.insight.98850
66. Seki E, De Minicis S, Osterreicher CH, Kluwe J, Osawa Y, Brenner DA, et al. TLR4 enhances TGF-beta signaling and hepatic fibrosis. Nat Med. 2007;13(11):1324-32. doi:10.1038/nm1663